AUCTORES
Globalize your Research

Journal of Surgical Case Reports and Images

Nan Lu1 *

Open Access

Research Article

Theoretical investigation on Brønsted acid-catalyzed cascade ring open-ing and double cyclization of 3-ethoxy cyclobutanone with naphthol to synthesize 2,8-dioxabicyclo [3.3.1] nonane

Nan Lu*, Chengxia Miao

College of Chemistry and Material Science, Shandong Agricultural University, Taian City 271018, Shandong Prov., P.R. China.

***Corresponding Author:** Nan Lu, Shandong Agricultural University, Taian City 271018, Shandong Prov., P.R. China.

Received Date: July 01, 2024; **Accepted Date:** July 12, 2024; **Published Date:** July 18, 2024

Citation: Nan Lu, Chengxia Miao, (2024), Theoretical investigation on Brønsted acid-catalyzed cascade ring open-ing and double cyclization of 3-ethoxy cyclobutanone with naphthol to synthesize 2,8-dioxabicyclo [3.3.1] nonane, *J, Surgical Case Reports and Images*, 7(6); **DOI:10.31579/2690-1897/202**

Abstract

The mechanism is investigated for cascade ring-opening/cyclization of 3-ethoxy 2-phenyl cyclobutanone with 2-naphthol leading to 2,8-dioxabicyclo[3.3.1]nonane. After protonation of carbonyl group, the nucleophilic attack of 2-naphthol prompts ring-opening of cyclobutanone. The enolization and ethanol removal generate alkenone with recovered naphthalene hydroxyl, which follows two possible pathways. In path A, another 2-naphthol facilitates Michael addition to render enol intermediate, which then affords desired product via dioxygen double cyclization containing three steps. In path B, the protonation from hydroxyl helps cyclization furnishing dihydropyrylium. With another deprotonated 2-naphthol, (3+3) annulation directly forms product and is more favorable than path A. Under the impact of Brønsted acid, positive (3+3) annulation is further improved with low barrier. The positive solvation effect is suggested by decreased absolute and activation energies in solution compared with in gas. These results are supported by Multiwfn analysis on FMO composition of specific TSs, and MBO value of vital bonding, breaking.

Keywords: Naphthol; ring-opening; cyclobutanone; (3+3) annulation; bicyclic ketal

1.Introduction

The 2,8-dioxabicyclo[3.3.1]nonanes are privileged members in numerous heterocyclic frameworks embedded with two oxygen atoms [1,2]. Since these bicyclic moieties constitute flavonoid compounds, they exhibit powerful anti-inflammatory, antiviral, antioxidant, and anticancer activities as several important drugs [3,4]. Characterized by rigid V-shaped diaryl-substituted structure, the construction of these bicyclic cores has received wide interest in recent years [5]. In this aspect, most methods and protocols require similar precursor of 2-hydroxy chalcones with different partners such as sequential knoevenagel condensation and hetero-Diels-Alder reaction in aqueous medium, cerium(III)-catalyzed domino approach using polyphenols and 1,4-Zwitterionic intermediates generated by regioselective cleavage of cyclobutane ring followed by their cycloaddition [6-8]. Then Zhu reported cationic-lanthanide-complex-catalyzed reaction with naphthols [9]. Wang developed controllable synthesis of two isomers 4H chromene under catalyst-free conditions [10]. Li achieved switchable synthesis of cyclohexanedione-fused 2,8-oxaza/2,8-dioxa bicyclo[3.3.1]nonanes by tunability of deamination/dehydration process [11].

The 1,4-zwitterionic intermediate generated from cleavage of C2−C3 bond was common before various ring opening, cycloaddition or rearrangement catalyzed by Lewis acid. In past few decades, many examples appeared such as intermolecular [4 + 2] cycloaddition of 3-alkoxycyclobutanone to aldehyde and ketone, synthesis of pyrazole through union of monosubstituted hydrazine with 3-ethoxycyclobutanone, total synthesis of (±)-aspidospermidine and regioselective inter-and intramolecular formal [4 + 2] cycloaddition of cyclo-butanone with indole, [3 + 3] annulation to construct pyrimidine and pyridine, between aromatic amine and 3-ethoxycyclobutanone to 2-lkylquinoline, remote site-selective Friedel-Crafts alkylation of β-Naphthol [12-17]. Okado achieved (±)-bremazocine, 2,3-di- or 2,3,3-trisubstituted N-Ts-2,3-dihydro-4-pyridone by using reaction of N-p-Toluenesulfonyl (Ts) aldimine with 3-ethoxycyclobutanone prompted by titanium(IV) chloride [18]. Lin reported diversity-oriented synthesis of bioactive pyridine-containing fused heterocycle through union of 3-ethoxycyclobutanone with various heterocyclic amine with excellent regioselectivity [19]. In despite of these progresses, activation of four-

membered ring via Brønsted acid (BA) is few. Only Xu obtained enantioselective Baeyer–Villiger oxidation of 3-substituted cyclobutanone giving γ-lactone [20].

However, it is still rare for direct ring-opening or cyclization with 3-ethoxy cyclobutanone catalyzed by BA. As far as we know, the development in recent years was Rahmatpour's regioselective synthesis of di-aromatic ring-fused 2,8-dioxa/dithia bicyclo[3,3,1]nonane via recyclable tandem formation of multiple chemical C-C/C-O and C-C/C-S bonds [21]. In this context, a breakthrough was Hazra's cascade ring-opening/cyclization of 3-ethoxy cyclobutanone [22]. Furthermore, this type of complex 15-membered macrocycle containing heteroatom was important biologically showing inhibitory and antitumor activities [23-25]. Although a range of 2,8-dioxabicyclo[3.3.1]nonane were obtained with various substituted naphthol, many problems still puzzled and there was no report about detailed mechanistic study explaining BA activation. What is the priority for carbonyl protonation of cyclobutanone and polarization of C2−C3 bond? How double cyclization is initiated from two oxygen atoms of two naphthols after Michael addition? Why (3+3) annulation with another 2-naphthol also possible from dihydropyrylium-type intermediate after cyclization from hydroxyl group? To solve these questions in experiment, an in-depth theoretical study was necessary for this strategy focusing on the competition of dioxygen-initiated double cyclization and (3+3) annulation.

2 Computational details

Optimized structures were obtained at M06-2X/6-31G(d) level of theory with GAUSSIAN09 [26]. In tests of popular DFT methods [27], M06-2X functional attained smaller standard deviation of difference between calculated value and experimental value in geometries than B3LYP including Becke's three-parameter hybrid functional combined with Lee−Yang−Parr correction for correlation [28,29]. The best compromise between accuracy and time consumption was provided with 6-31G(d) basis set on energy calculations. Also, M06-2X functional was found to give relatively accurate results for catalysed enantioselective (4 + 3), concerted [4 + 2], stepwise (2 + 2) cycloaddition and catalysed Diels−Alder reactions [30,31]. Together with the best performance on noncovalent interaction, M06-2X functional is believed to be suitable for this system [32-34]. The nature of each structure was verified by performing harmonic vibrational frequency calculations. Intrinsic reaction coordinate (IRC) calculations were examined to confirm the right connections among key transition-states and corresponding reactants and products. Harmonic frequency calculations were carried out at the M06-2X/6-31G(d) level to gain zero-point vibrational energy (ZPVE) and thermodynamic corrections at 298.15 K and 1 atm for each structure in toluene.

The solvation-corrected free energies were obtained at the M06-2X/6-311++G(d,p) level by using integral equation formalism polarizable continuum model (IEFPCM) in Truhlar's "density" solvation model [35-39] on the M06-2X/6-31G(d)-optimized geometries. As an efficient method obtaining bond and lone pair of a molecule from modern ab initio wave functions, NBO procedure was performed with Natural bond orbital (NBO3.1) to characterize electronic properties and bonding orbital interactions [40-42]. The wave function analysis was provided using Multiwfn_3.7_dev package [43] including research on frontier molecular orbital (FMO) and Mayer bond order (MBO).

3 Results and Discussion

The mechanism was explored for BA-catalyzed cascade ring-opening/cyclization of 3-ethoxy 2-phenyl cyclobutanone 1 with 2-naphthol 2 leading to 2,8-dioxabicyclo [3.3.1] nonane 3 (Scheme 1). Illustrated by black arrow of Scheme 2, initially the carbonyl group protonation of 1 polarize the C2−C5 bond. Then via the nucleophilic attack of 2 at C2 center, the ring-opening of 1 happen leading to intermediate I. Eventually the enolization and removal of ethanol generate intermediate II, which follows two possible pathways. In path A, another molecule 2 facilitates Michael addition to render intermediate III, which then affords desired product 3 via double cyclization from two oxygen atoms of two molecules of 2 (red arrow). In path B, the protonation of II carbonyl group by hydroxyl of 2 facilitates cyclization furnishing dihydropyrylium. Subsequently, a (3+3) annulation with another deprotonated 2 leads to product 3 (blue arrow). Under the impact of BA the positive (3+3) annulation takes place via three steps (green arrow). The schematic structures of optimized TSs in Scheme 2 were listed by Figure 1. The activation energy was shown in Table 1 for all steps. Supplementary Table S1, Table S2 provided the relative energies of all stationary points. According to experiment, the Gibbs free energies in methanol solution phase are discussed here.

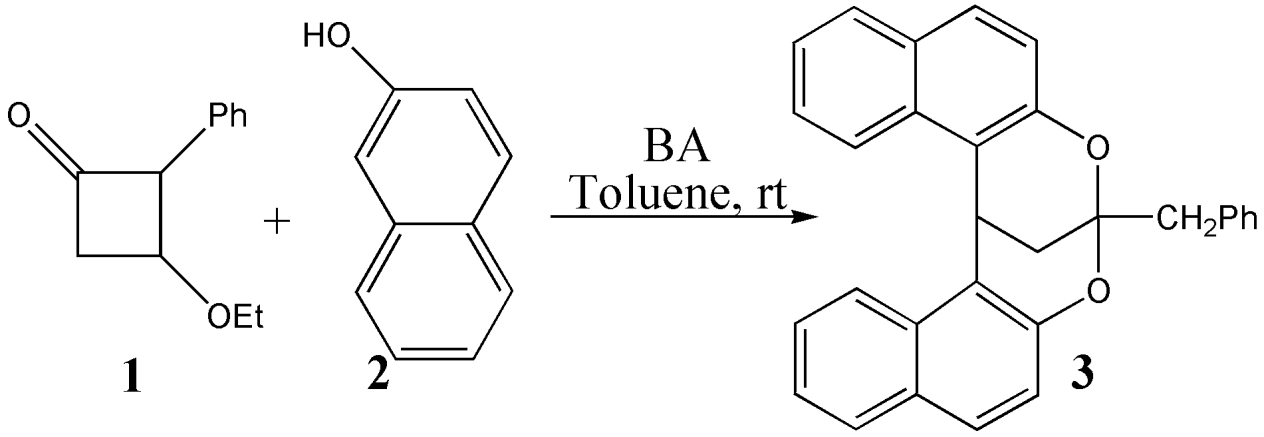

Scheme 1 (a) Brønsted acid (BA)-catalyzed cascade ring-opening/cyclization of 3-ethoxy 2-phenyl cyclobutanone **1** with 2-naphthol **2** leading to 2,8-dioxabicyclo [3.3.1] nonane **3**.

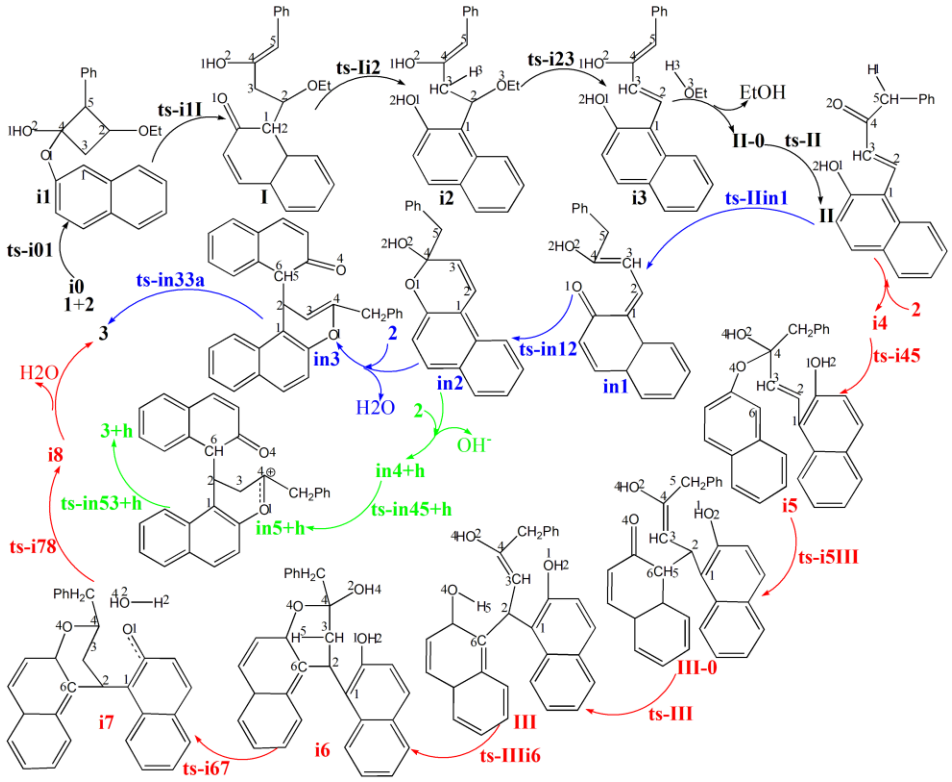

Scheme 2: Proposed reaction mechanism of BA-catalyzed cascade ring-opening/cyclization of **1** with **2** leading to **3**. TS is named according to the two intermediates it connects.

TS	$\Delta G^{\neq}_{gas}$	$\Delta G^{\neq}_{sol}$
ts-i01	19.9	15.7
ts-i1I	29.2	26.8
ts-Ii2	28.3	25.5
ts-i23	18.7	16.3
ts-II	22.5	21.7
ts-i45	18.2	15.5
ts-i5III	9.6	6.7
ts-III	26.7	23.4
ts-IIIi6	12.3	9.2
ts-i67	30.8	27.3
ts-i78	31.1	29.5
ts-IIin1	11.8	10.2
ts-in12	20.5	18.1
ts-in33	26.0	23.3
ts-in45h+	10.2	7.8
ts-in53h+	2.4	3.3

Table 1: The activation energy (in kcal mol^{-1}) of all reactions in gas and solvent

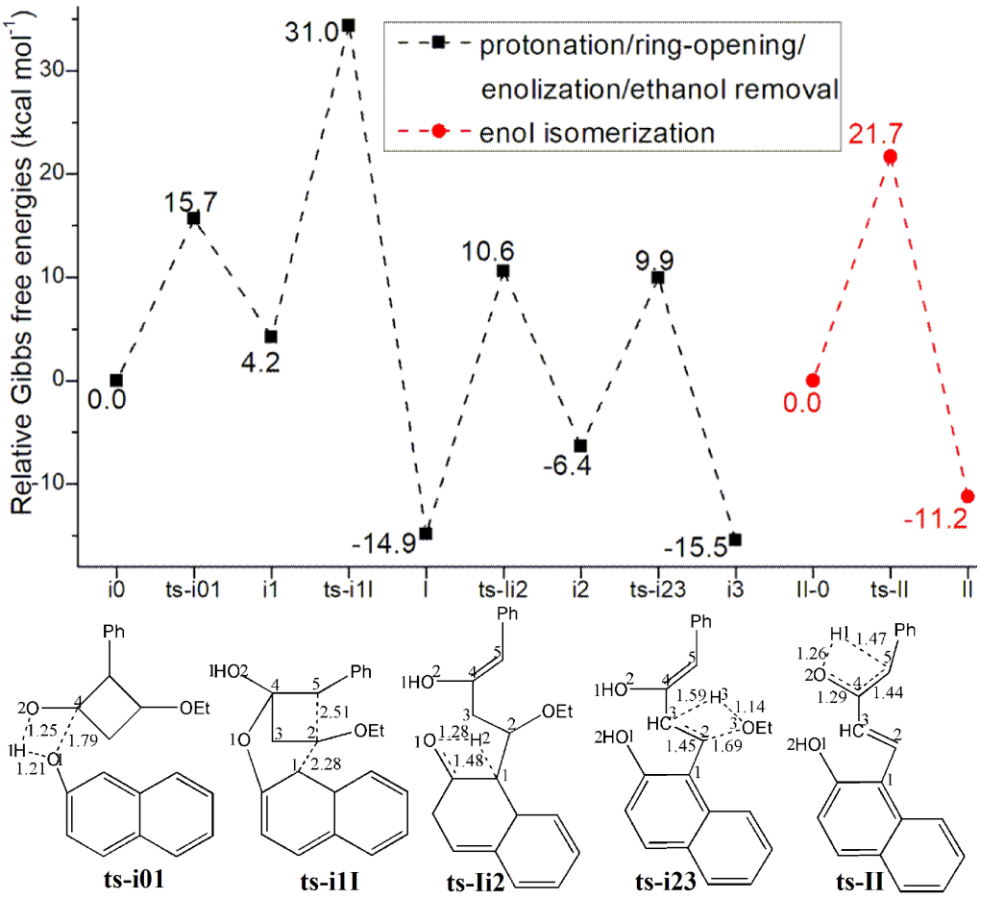
Relative Gibbs free energies (kcal mol-1)
protonation/ring-opening/
enolization/ethanol removal
enol isomerization
31.0
15.7
4.2
0.0
-14.9
10.6
-6.4
9.9
-15.5
21.7
0.0
-11.2
i0
ts-i01
i1
ts-i1I
I
ts-Ii2
i2
ts-i23
i3
II-0
ts-II
II
ts-i01
ts-i1I
ts-Ii2
ts-i23
ts-II

(b)

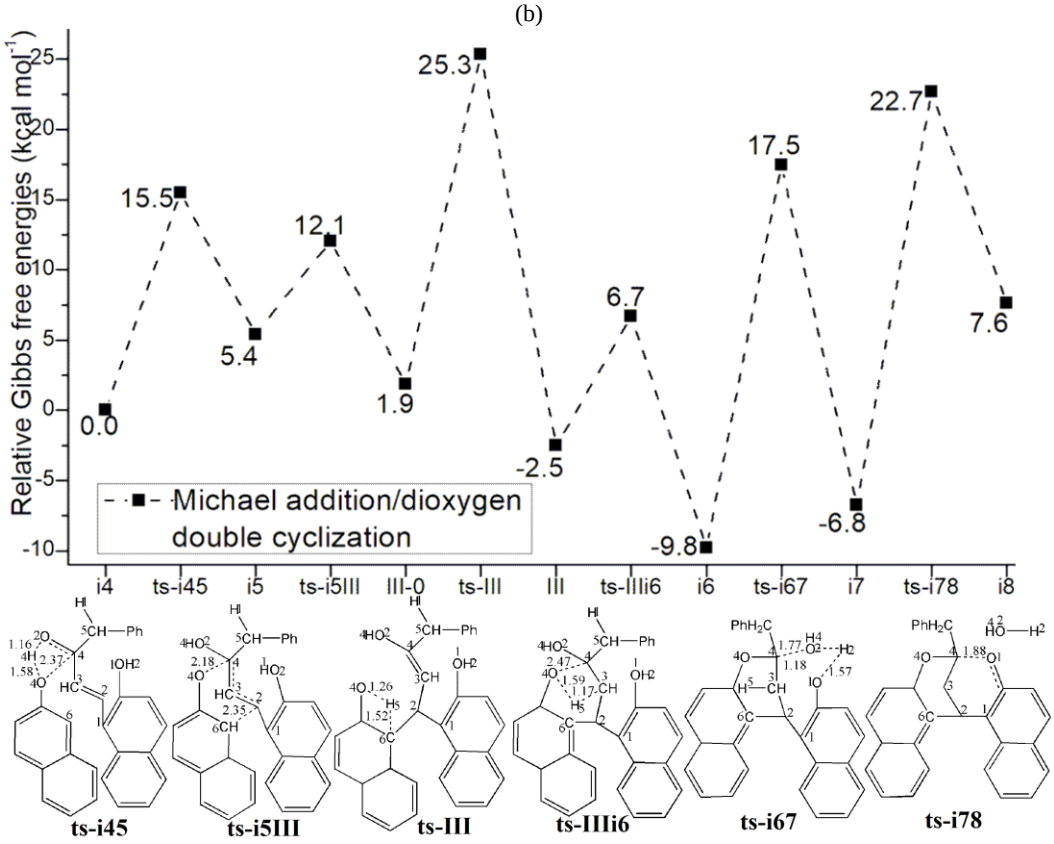
Relative Gibbs free energies (kcal mol-1)
Michael addition/dioxygen
double cyclization
0.0
15.5
5.4
12.1
1.9
25.3
-2.5
6.7
-9.8
17.5
-6.8
22.7
7.6
i4
ts-i45
i5
ts-i5III
III-0
ts-III
III
ts-IIIi6
i6
ts-i67
i7
ts-i78
i8
ts-i45
ts-i5III
ts-III
ts-IIIi6
ts-i67
ts-i78

(c)

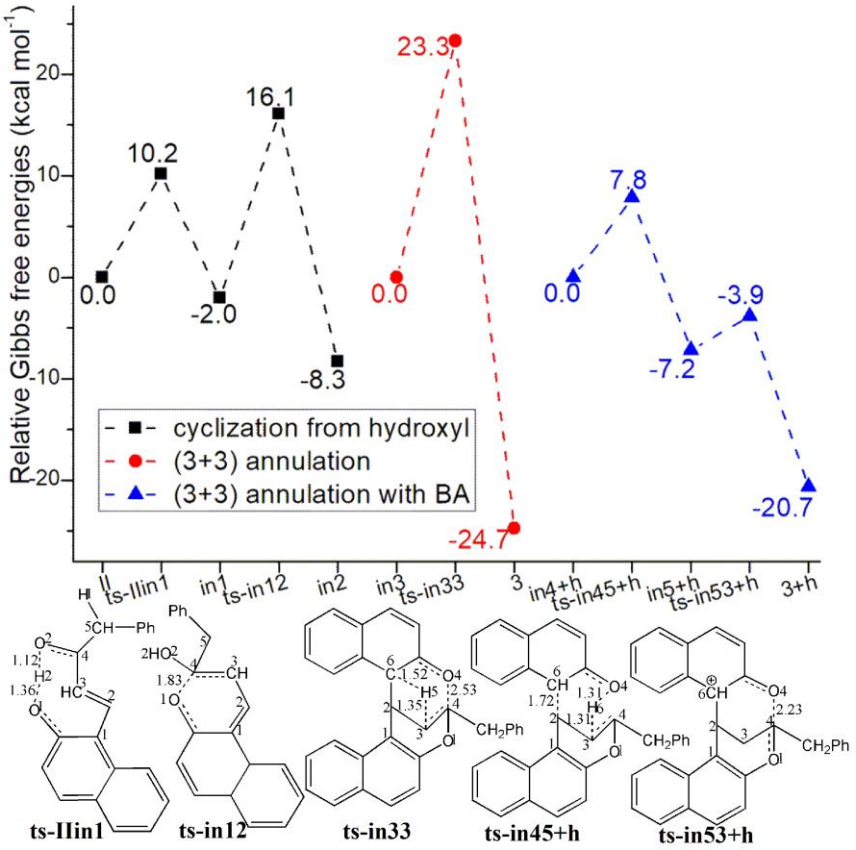

3.1 Protonation/ring-opening/enolization/ethanol removal and enol isomerization

Initially the complex of 1 and 2 denoted as i0, the carbonyl group of 1 is protonated by hydroxyl of 2 polarizing the C2−C5 bond. This process proceeds via ts-i01 as step 1 with the activation energy of 15.7 kcal mol^{-1} relative to the starting point i0 endothermic by 4.2 kcal mol^{-1} (black dash line of Figure 1a). The transition vector includes the transfer of H1 from O1 to O2 and the closing of O1 to C4 makes it changing from sp2 hybrid to sp3 (1.21, 1.25, 1.79 Å) (Figure S1a). Without proton, the reactive hydroxyl O1 is bonded to sp3 C4 in resultant i1, from which the ring-opening of 1 happen under the nucleophilic attack of 2 at C2 center leading to intermediate I. As step 2, this occurs via ts-i1I with activation energy of 26.8 kcal mol^{-1} exothermic by -14.9 kcal mol^{-1}. The transition vector contains cleavage of C2⋯C5 and concerted linkage of C1⋯C2 (2.28, 2.51 Å). Therefore I is stable after releasing the tension of quadruple ring of 1. While once bonded to C2, the C1 turns to be sp3 hybrid breaking the conjugation of naphthalene ring apt to kick off a hydrogen in following process.

Then the enolization of carbonyl O1 takes place via ts-Ii2 in subsequent step 3 with activation energy of 25.5 kcal mol^{-1} affording i2 exothermic by -6.4 kcal mol^{-1}. According to the transition vector, the proton H2 is transferring from C1 to O1, which is recovered to hydroxyl group O1H2. In next step 4, the OEt bonded to C2 and H on C3 are disconnected simultaneously and assemble stable EtOH molecule leaving from the system. Via ts-i23, ethanol is removed with a barrier of 16.3 kcal mol^{-1} exothermic by -15.5 kcal mol^{-1} delivering intermediate i3. The transition vector corresponds to the elongation of C2-O3, C3-H3 single bond to dissociation and bonding of O3-H3, C2-C3 shortened from single to double one at the same time (1.69, 1.59, 1.14, 1.45 Å) (Figure S1b).

Without ethanol, the intermediate II-0 is taken as new starting point of step 5 (red dash line of Figure 1a). The O2H1 hydroxyl group formed in step 1 denotes H1 to sp2 C5 to complete enol tautomerism. This happens via ts-II with activation energy of 21.7 kcal mol^{-1} exothermic by -11.2 kcal mol^{-1} yielding intermediate II more stable. The transition vector suggests remarkable O2⋯H1⋯C5 shifting as well as C4-C5 stretching from double bond to single.

3.2 Michael addition/dioxygen double cyclization

Two pathways are possible from II. In path A (black dash line of Figure 1b), the addition of another molecule 2 forms complex i4 as starting point of the following six steps. As preparation of Michael addition, the step 6 takes place via ts-i45 with activation energy of 15.5 kcal mol^{-1} forming reactive i5 endothermic by 5.4 kcal mol^{-1}. Similar with ts-i01, the carbonyl O2 is protonated by new naphthyl hydroxyl O4H4. According to the transition vector, the atomic motion is composed of O4⋯H4⋯O2 proton shifting and laggered approaching of O4⋯C4 (1.58, 1.16, 2.37 Å). This greatly facilitate the crucial Michael addition seen from the low barrier via hexagonal ring structure of ts-i5III. Seen from the detailed motion demonstrated by its transition vector (Figure S1c), the departure of O4-C4 bond is accompanied by formation of C6-C2 bond (2.18, 2.35 Å). Clearly, the cleavage of O4-C4 endows negative charge concentrated on O4, passes on to C6 and enhance its nucleophilic ability. Likewise, the ability of C2 as an electrophilic center is also increased. Hence the small activation energy of step 7 is only 6.7 kcal mol^{-1} endothermic by 1.9 kcal mol^{-1} giving III-0, which is lower than former i5 in relative energy yet still reactive to initiate next step.

In step 8, III-0 undergoes carbonyl enolization of the second 2 via ts-III just like ts-Ii2 with activation energy of 23.4 kcal mol^{-1} exothermic by -2.5 kcal mol^{-1} generating III favorable in thermodynamics. The transition vector of this second enolization is about proton transfer of C6⋯H5⋯O4 (1.52, 1.26 Å), which not only recovers hydroxyl O4H5 but turns sp3 C6 in III-0 to be sp2 stable conjugated structure of naphthalene ring in III. From III, the desired product 3 is produced via double cyclization from two oxygen of two 2 molecule through three steps. The first nucleophilic attack of O4 to C4 proceeds via ts-IIIi6 followed by proton H5 given by O4 to C3 concertedly. This can be illustrated in detail by the transition vector (1.59, 1.17, 2.47 Å), which makes C3 methylene on the one hand

and improves the nucleophilic ability of O4 on the other. The activation energy of step 9 is 9.2 kcal mol^{-1} exothermic by -9.8 kcal mol^{-1} relative to III.

Before the second nucleophilic addition of O1 to C4, the dehydration is located via ts-i67 with activation energy of 27.3 kcal mol^{-1} exothermic by -6.8 kcal mol^{-1} as step 10. This is also belongs to small molecule H_2O assembling and then leaving process similar to the case of EtOH removal via ts-i23. Here, the O2H4 on C4 combines with H2 on O1 as one water (1.77, 1.57, 1.18 Å) (Figure S1d) in resulting i7, which is stable although O1 and C4 is not yet connected owing to the distance. The real O1-C4 single bond should be achieved in last step 11 via ts-i78 with activation energy of 29.5 kcal mol^{-1} endothermic by 7.6 kcal mol^{-1} only involving simple O1···C4 approaching (1.88 Å). The barrier is somewhat high due to the need of overcoming tension generated by spatial distance.

Ultimately, the third simple step of dioxygen double cyclization is determined to be rate-limiting for path A. To highlight the idea of feasibility for changes in electron density and not molecular orbital interactions are responsible of the reactivity of organic molecules, quantum chemical tool Multiwfn was applied to analyze of electron density such as MBO results of bonding atoms and contribution of atomic orbital to HOMO of typical TSs (Table S3, Figure S2). These results all confirm the above analysis.

3.3 Cyclization from hydroxyl/(3+3) annulation and BA impact

In path B, the carbonyl O2 can also be protonated by original hydroxyl O1H2 from II via ts-IIin1 in step 6 with a barrier of 10.2 kcal mol^{-1} exothermic by -2.0 kcal mol^{-1}delivering in1. The transition vector corresponds to simple proton H2 transfer from O1 to O2 (1.36, 1.12 Å) (Figure S1e). This faciliates first cyclization from O1 to C4 via ts-in12 as step 7 with the activation energy of 18.1 kcal mol^{-1} relative to in1 exothermic by -8.3 kcal mol^{-1} (black dash line of Figure 1c). Therefore the difficult nucleophilic addition of O1 to C4 in path A becomes readily accessible in path B, which is approved by the transition vector of ts-in12.

After the removal of O2H2 from cyclization product in2, a dihydropyrylium is obtained, which is easily binding the second deprotonated 2 via C6-C2 bond forming in3 as new starting point of subsequent step 3 (red dash line of Figure 1c). The second cyclization from O4 to C4 occurs via ts-in33 with activation energy of 23.3 kcal mol^{-1} by exothermic -24.7 kcal mol^{-1} directly leading to 3. The transition vector reveals a concerted asynchronous process containing previous C3 methylenation by C6 via C6···H5···C3 atomic motion and O4···C4 linking afterwords (1.52, 1.35, 2.53 Å) (Figure S1f). Evidently for path B, (3+3) annulation includes two steps with the second concerted one as rate-limiting more favorable than that of path A from kinetics.

The impact of BA are also considered for preferential (3+3) annulation modeled as a system with one positive charge (blue dash line of Figure 1c). The initial complex binding dihydropyrylium and neutral 2 denoted as in4+h is taken as starting point of the next two steps. The subsequent step 3 takes place via ts-in45+h with activation energy of 7.8 kcal mol^{-1} affording in5+h exothermic by -7.2 kcal mol^{-1}, where C3 is methylenated by O4 via O4···H6···C3 and C6···C2 is bonding in concerted mode. Then via ts-in53+h with a rather low barrier of 3.3 kcal mol^{-1}, O4-C4 single bond is accomplished in step 4 delivering 3+h exothermic by -20.7 kcal mol^{-1} as precusor of 3. Assisted by BA, the (3+3) annulation becomes easier involving three steps with the first O1···C4 bonding as rate-limiting comparatively.

4 Conclusions

Our DFT calculations provide the first theoretical investigation on cascade ring-opening/cyclization of 3-ethoxy 2-phenyl cyclobutanone with 2-naphthol leading to 2,8-dioxabicyclo[3.3.1]nonane. The carbonyl group of cyclobutanone is initially protonated by hydroxyl of 2-naphthol, the nucleophilic attack of which prompts ring-opening of cyclobutanone. The subsequent enolization and removal of ethanol generate alkenone intermediate with recovered naphthalene hydroxyl, which follows two possible pathways. In path A, another 2-naphthol facilitates Michael addition to render enol intermediate, which then affords desired product via dioxygen double cyclization containing three steps with the third simple O1···C4 approaching as rate-limiting. The barrier is somewhat high due to the tension generated by spatial distance yet readily to overcome under room temperature. In path B, the protonation from hydroxyl helps cyclization furnishing dihydropyrylium. With another deprotonated 2-naphthol, (3+3) annulation includes two steps with the second concerted O4···C4 bonding and C3 methylenation by C6 as rate-limiting, which directly forms product and is more favorable than path A from kinetics. Under the impact of BA the positive (3+3) annulation involves three steps with the first O1···C4 bonding as rate-limiting comparatively. The positive solvation effect is suggested by decreased absolute and activation energies in toluene solution compared with in gas. These results are supported by Multiwfn analysis on FMO composition of specific TSs, and MBO value of vital bonding, breaking.

Electronic Supplementary Material

Supplementary data available: [Computation information and cartesian coordinates of stationary points; Calculated relative energies for the ZPE-corrected Gibbs free energies (ΔG_{gas}), and Gibbs free energies (ΔG_{sol}) for all species in solution phase at 298 K.]

Author contributions: Conceptualization, Nan Lu; Methodology, Nan Lu; Software, Nan Lu; Validation, Nan Lu; Formal Analysis, Nan Lu; Investigation, Nan Lu; Resources, Nan Lu; Data Curation, Nan Lu; Writing-Original Draft Preparation, Nan Lu; Writing-Review & Editing, Nan Lu; Visualization, Nan Lu; Supervision, Chengxia Miao; Project Administration, Chengxia Miao; Funding Acquisition, Chengxia Miao. All authors have read and agreed to the published version of the manuscript.

Funding: This work was supported by National Natural Science Foundation of China (21972079) and Key Laboratory of Agricultural Film Application of Ministry of Agriculture and Rural Affairs, P.R. China.

Conflict of interest: The authors declare no conflict of interest.

References

1. Ishida, N.; Murakami, M. (2021). Cleavage of Carbon-Carbon σ- Bonds of Four Membered Rings. Chem. Rev., 121, 264−299.
2. Ghosh, A.; Dey, R.; Banerjee, P. (2021). Relieving the stress together: annulation of two different strained rings towards the formation of biologically significant heterocyclic scaffolds. Chem. Commun. 57, 5359−5373.
3. Xu, M. F.; Shen, L. Q.; Wang, K. W. (2009). A new biflavonoid from Daphniphyllum angustifolium Hutch. Fitoterapia.80, 461−464.
4. Nakashima, K. I.; Abe, N.; Kamiya, F.; Ito, T.; Oyama, M.; et al. (2009). Novel Flavonoids in Dragons Blood of Daemonorops draco. Helv. Chim. Acta, 92, 1999−2008.
5. Yin, G.; Ren, T.; Rao, Y.; Zhou, Y.; Li, Z. et al. (2013). Stereoselective Synthesis of 2,8-Dioxabicyclo[3.3.1]nonane Derivatives via a Sequential Michael Addition/Bicyclizatio Reaction. *J. Org. Chem*. 78, 3132−3141.
6. Srinivas, V.; Koketsu, M. (2013). Synthesis of 2,8-Dioxabicyclo[3.3.1]nonane Derivatives via a Sequential Knoevenagel Condensation and Hetero-Diels-Alder Reaction in an Aqueous Medium. *J. Org. Chem*., 78, 11612−11617.
7. Chand Ganguly, N.; Roy, S.; Mondal, P. (2014). Cerium(III)-catalyzed regioselective coupling of 2- hydroxychalcones and polyphenols: an efficient domino approach towards synthesis of novel dibenzo-2,8-dioxabicyclo[3.3.1]-nonanes. RSC Adv. 4,

42078−42086.

8. Matsuo, J. (2014). 1,4-Zwitterionic intermediates formed by cleavage of a cyclobutane ring and their cycloaddition reactions. Tetrahedron Lett.55, 2589-2595.
9. Zhu, Y.; Yao, Z.; Xu, F. (2018). Cationic-lanthanide-complex-catalyzedreactionof2-hydroxychalcones with naphthols: Facile synthesis of 2,8-dioxabicyclo [3.3.1]nonanes. Tetrahedron. 74, 4211−4219.
10. Wang, S.; Lin, J.-J.; Cui, X.; Li, J.-P.; Huang, C. (2021). Controllable Synthesis of Two Isomers 4H Chromene and 2,8-Dioxabicyclo[3.3.1]-nonane Derivatives under Catalyst-Free Conditions. J. Org. Chem. 86, 16396−16408.
11. Li, J.; Wang, S.; Xu, G.; Cui, X.; Zi, B.; Liu, T.; Huang, C. (2022). Switchable Synthesis of Cyclohexanedione-fused 2,8-Oxaza/2,8-Dioxa Bicyclo[3.3.1]nonanes and 4-Substituted 4H-Chromenes by Tunability of the Deamination/Dehydration Process. Asian J. Org. Chem. 11, No. e202100797.
12. Sasaki, S.; Tanaka, H.; Ishibashi, H.; Matsuo, J. (2008). Lewis Acid Catalyzed Intermolecular [4 + 2] Cycloaddition of 3-Alkoxycyclobutanones to Aldehydes and Ketones. J. Am. Chem. Soc. 130, 11600−11601.
13. Shan, G.; Liu, P.; Rao, Y. (2011). A New Synthesis of Pyrazoles through a Lewis Acid Catalyzed Union of 3-Ethoxycyclobutanones with Monosubstituted Hydrazines. Org. Lett. 13, 1746−1749.
14. Kawano, M.; Kiuchi, T.; Negishi, S.; Tanaka, H.; Hoshikawa, T. et al. (2013). Regioselective Inter-and Intramolecular Formal [4 + 2] Cycloaddition of Cyclo-butanones with Indoles and Total Synthesis of (±)-Aspidospermidine. Angew. Chem., Int. Ed, 52, 906−910.
15. Zhou, Y.; Tang, Z.; Song, Q. (2017). Lewis Acid-Mediated [3 + 3] Annulation for the Construction of Substituted Pyrimidine and Pyridine Derivatives. Adv. Synth. Catal, 359, 952−958.
16. Shan, G.; Sun, X.; Xia, Q.; Rao, Y. (2011). A Facile Synthesis of Substituted 2-Alkylquinolines through [3 + 3] Annulation between 3-Ethoxycyclobutanones and Aromatic Amines at Room Temperature. Org. Lett. 13, 5770−5773.
17. Hazra, A.; Kanji, T.; Banerjee, P. (2023). Merging Two Strained Carbocycles: Lewis Acid Catalyzed Remote Site-Selective Friedel-Crafts Alkylation of in Situ Generated β-Naphthol. *J. Org. Chem*. 88, 960−971.
18. Okado, R.; Ishibashi, H.; Matsuo, J. (2010). A New Synthesis of 2,3-Di- or 2,3,3-Trisubstituted 2,3-Dihydro-4-pyridonesby Reaction of 3-Ethoxycyclobutanones and N-p-Toluenesulfonyl Imines Using Titanium(IV) Chloride: Synthesis of (±)-Bremazocine. Org. Lett. 12, 3266−3268.
19. Lin, Y.; Yang, X.; Pan, W.; Rao, Y. (2016). One-Step Synthesis of Diverse Pyridine-Containing Heterocycles with 3-Ethoxycyclobutanones at Room Temperature. Org. Lett. 18, 2304−2307.
20. Xu, S.; Wang, Z.; Zhang, X.; Zhang, X.; Ding, K. (2008). Chiral Brønsted Acid Catalyzed Asymmetric Baeyer−Villiger Reaction of 3-Substituted Cyclobutanones by Using Aqueous H2O2. Angew. Chem., Int. Ed. 47, 2840−2843.
21. Rahmatpour, A.; Sajjadinezhad, S. M.; Mirkani, A.; Notash, B. (2021). Regioselective synthesis of di-aromatic ring-fused 2,8-dioxa/dithia bicyclo[3,3,1]nonane derivatives via recyclable polymeric Brønsted acid-catalyzed one-pot tandem formation of multiple chemical C-C/C-O and C-C/C-S bonds. Tetrahedron. 95, 132341.
22. Hazra, A.; Kanji, T.; Banerjee, P. Brønsted Acid-Catalyzed Cascade Ring-Opening/Cyclization of 3-Ethoxy Cyclobutanones to Access 2,8-Dioxabicyclo[3.3.1]nonane Derivatives. *J. Org. Chem*. DOI: 10.1021/acs.joc.4c00344
23. Bonazzi, S.; Cheng, B.; Wzorek, J. S.; Evans, D. A. (2013). Total Synthesis of (−)-Nakadomarin A. *J. Am. Chem*. Soc. 135, 9338−9341.
24. Pota, K.; Molnar, E.; Kalman, F. K.; Freire, D. M.; Tircsó, G.; Green, K. N. (2020). Manganese Complex of a Rigidified 15-Membered Macrocycle: A Comprehensive Study. Inorg. Chem, 59, 11366−11376.
25. Shimizu, T.; Takahashi, N.; Huber, V. J.; Asawa, Y.; Ueda, H.et al. (2021). Design and synthesis of 14 and 15-membered macrocyclic scaffolds exhibiting inhibitory activities of hypoxia-inducible factor 1α. *Bioorg. Med. Chem*. 30, 115949.
26. Frisch, M. J.; Trucks, G. W.; Schlegel, H. B. et al. (2010). Gaussian 09 (Revision B.01), Gaussian, Inc., Wallingford, CT.
27. Stephens, P. J.; Devlin, F. J.; Chabalowski, C. F.; Frisch, M. J. (1994). Ab initio Calculation of Vibrational Absorption and Circular Dichroism Spectra Using Density Functional Force Fields, *J. Phys. Chem*. 98, 11623-11627.
28. Becke, A. D. (1996). Density-functional thermochemistry. IV. A new dynamical correlation functional and implications for exact-exchange mixing. *J. Chem. Phys*. 104, 1040-1046.
29. Lee, C. T.; Yang,W. T.; Parr, R. G. (1988). Development of the Colle-Salvetti correlation-energy formula into a functional of the electron density. Phys. Rev. B, 37, 785-789.
30. Li, X.; Kong, X.; Yang, S.; Meng, M.; Zhan, X. et al. (2019). Bifunctional Thiourea-Catalyzed Asymmetric Inverse-Electron-Demand Diels-Alder Reaction of Allyl Ketones and Vinyl 1,2-Diketones via Dienolate Intermediate, Org. Lett, 21, 1979-1983.
31. Krenske, E. H.; Houk, K. N.; Harmata, M. (2015). Computational Analysis of the Stereochemical Outcome in the Imidazolidinone-Catalyzed Enantioselective (4 + 3)-Cycloaddition Reaction, *J. Org. Chem*. 2015, 80, 744-750.
32. Lv, H.; Han, F.; Wang, N.; Lu, N.; Song, Z. et al. (2022). Ionic Liquid Catalyzed C-C Bond Formation for the Synthesis of Polysubstituted Olefins. Eur. *J. Org. Chem*. e202201222.
33. Zhuang, H.; Lu, N.; Ji, N.; Han, F.; Miao, C. (2021). Bu4NHSO4-Catalyzed Direct N-Allylation of Pyrazole and its Derivatives with Allylic Alcohols in Water: A Metal-free, Recyclable and Sustainable System. *Advanced Synthesis & Catalysis* , 363, 5461-5472.
34. Lu, N.; Liang, H.; Qian, P.; Lan, X.; Miao, C. (2020). Theoretical investigation on the mechanism and enantioselectivity of organocatalytic asymmetric Povarov reactions of anilines and aldehydes. *Int. J. Quantum Chem*. 120, e26574.
35. Tapia, O. (1992). Solvent effect theories: Quantum and classical formalisms and their applications in chemistry and biochemistry. *J. Math. Chem*. 10, 139-181.
36. Tomasi, J.; Persico, M. (1994). Molecular Interactions in Solution: An Overview of Methods Based on Continuous Distributions of the Solvent. *Chem.* Rev. 94, 2027-2094.
37. Simkin, B. Y.; Sheikhet, I. (1995). Quantum Chemical and Statistical Theory of Solutions—A Computational Approach, Ellis Horwood, London .
38. Tomasi, J.; Mennucci, B.; Cammi, R. (2005). Quantum Mechanical Continuum Solvation Models. Chem. Rev. 105, 2999-3093.
39. Marenich, A. V.; Cramer, C. J.; Truhlar, D. G. (2009). Universal Solvation Model Based on Solute Electron Density and on a Continuum Model of the Solvent Defined by the Bulk Dielectric Constant and Atomic Surface Tensions. *J. Phys. Chem*. B,113, 6378–6396.
40. Reed, A. E.; Weinstock, R. B.; Weinhold, F. (1985). Natural population analysis. *J. Chem. Phys*. 83, 735-746.
41. Reed, A. E.; Curtiss, L. A.; Weinhold, F. (1988). Intermolecular interactions from a natural bond orbital donor-acceptor view point. Chem. Rev. 88, 899-926.
42. Foresman, J. B.; Frisch, A. (1996). Exploring Chemistry with

Electronic Structure Methods, 2nd ed., Gaussian, Inc., Pittsburgh.

43. Lu, T.; Chen, F. (2012). Multiwfn: A multifunctional wavefunction analyzer. *J. Comput. Chem.* 33, 580-592.

DOI:10.31579/2690-1897/202

Supplementary Information

Software: GAUSSIAN09
Level of Theory: M06-2X
Basis Set: 6-31G(d)
Geometry [Cartesian coordinates]:
Optimized Cartesian coordinates for **ts-i01**

Center Number	Atomic Number	Atomic Type	Coordinates (Angstroms) X	Y	Z
1	6	0	0.714191	-0.716605	-0.614145
2	6	0	0.171751	0.461533	-1.397049
3	6	0	1.513431	1.160151	-1.083744
4	6	0	1.760568	0.150788	0.096020
5	8	0	0.912013	-1.913047	-1.080347
6	8	0	1.362079	2.508328	-0.758466
7	6	0	3.671374	2.940002	-0.029651
8	6	0	2.517443	3.305810	-0.950575
9	1	0	-0.637004	0.978010	-0.869155
10	1	0	-0.101964	0.268703	-2.434922
11	1	0	2.255516	1.016414	-1.882500
12	1	0	1.314144	0.602377	0.988154
13	1	0	4.473412	3.678700	-0.122758
14	1	0	4.086046	1.956956	-0.271533
15	1	0	3.334227	2.921568	1.011581
16	1	0	2.185131	4.330336	-0.762912
17	1	0	2.835246	3.243548	-2.002885
18	6	0	3.113871	-0.421563	0.372237
19	6	0	3.717700	-0.256475	1.621201
20	6	0	3.813913	-1.102000	-0.630300
21	6	0	4.996373	-0.748818	1.865055
22	1	0	3.179935	0.268469	2.407193
23	6	0	5.092179	-1.593666	-0.388105
24	1	0	3.343160	-1.265799	-1.595180
25	6	0	5.688572	-1.416703	0.858687
26	1	0	5.451611	-0.609641	2.840983
27	1	0	5.622590	-2.122010	-1.174528
28	1	0	6.686376	-1.801948	1.045274
29	6	0	-6.485484	0.640054	0.147059
30	6	0	-5.799555	-0.285319	-0.597072
31	6	0	-4.442529	-0.584192	-0.311196
32	6	0	-3.796706	0.087759	0.764803
33	6	0	-4.532758	1.040125	1.517995
34	6	0	-5.842780	1.309852	1.216392
35	1	0	-4.197799	-2.042012	-1.892489
36	1	0	-7.523066	0.863341	-0.080567
37	1	0	-6.285509	-0.803587	-1.419760
38	6	0	-3.704254	-1.533064	-1.068736
39	6	0	-2.441057	-0.212590	1.055537
40	1	0	-4.037190	1.551961	2.338620
41	1	0	-6.394921	2.041030	1.798812
42	6	0	-1.762389	-1.139659	0.304919
43	6	0	-2.394659	-1.804964	-0.778985
44	1	0	-1.932870	0.282806	1.877980
45	1	0	-1.820270	-2.517475	-1.364028
46	8	0	-0.443948	-1.387730	0.575664
47	1	0	0.106890	-2.184897	-0.152284

Optimized Cartesian coordinates for **ts-i1I**

Center Number	Atomic Number	Atomic Type	Coordinates (Angstroms) X	Y	Z
1	6	0	0.241546	-1.530062	-0.697665
2	6	0	0.473489	-1.270731	-2.187094

3	6	0	1.152480	0.030012	-2.455431
4	6	0	1.322805	-1.327704	0.264198
5	8	0	-0.349834	-2.799781	-0.639471
6	8	0	0.947629	0.502163	-3.654056
7	6	0	2.602268	2.383949	-3.712199
8	6	0	2.081642	1.111763	-4.327473
9	1	0	-0.494418	-1.201299	-2.695825
10	1	0	1.037780	-2.072304	-2.668945
11	1	0	2.120819	0.223027	-1.994469
12	1	0	1.064101	-0.797348	1.176613
13	1	0	2.986022	2.216589	-2.702167
14	1	0	1.821777	3.142605	-3.680879
15	1	0	3.425801	2.756442	-4.328696
16	1	0	1.703587	1.280366	-5.335838
17	1	0	2.855777	0.337975	-4.372147
18	6	0	2.586330	-1.915761	0.111523
19	6	0	3.677394	-1.543704	0.964948
20	6	0	2.917771	-2.844872	-0.924629
21	6	0	4.956135	-2.022287	0.773576
22	1	0	3.472656	-0.857592	1.785027
23	6	0	4.214229	-3.309221	-1.104961
24	1	0	2.117436	-3.257405	-1.533578
25	6	0	5.257501	-2.903091	-0.276246
26	1	0	5.745420	-1.702239	1.450466
27	1	0	4.408339	-4.023161	-1.903158
28	1	0	6.267616	-3.269266	-0.425337
29	6	0	0.198201	5.475731	-2.010556
30	6	0	-0.882111	4.642399	-2.212074
31	6	0	-0.845031	3.301175	-1.778365
32	6	0	0.327900	2.790327	-1.193002
33	6	0	1.402242	3.664313	-0.959856
34	6	0	1.340914	4.987294	-1.358141
35	1	0	-2.907022	2.857973	-2.296648
36	1	0	0.157007	6.511660	-2.331218
37	1	0	-1.789687	5.017140	-2.678580
38	6	0	-1.995649	2.453826	-1.863273
39	6	0	0.398503	1.393268	-0.786742
40	1	0	2.284854	3.285950	-0.450814
41	1	0	2.183410	5.646585	-1.174177
42	6	0	-0.791117	0.647263	-0.791072
43	6	0	-1.978991	1.191548	-1.360982
44	1	0	1.191430	1.107909	-0.112962
45	1	0	-2.850421	0.546585	-1.392890
46	8	0	-0.896857	-0.618856	-0.422683
47	1	0	-0.075346	-3.154591	0.219700

Optimized Cartesian coordinates for **ts-Ii2**

Center Number	Atomic Number	Atomic Type	Coordinates (Angstroms) X	Y	Z
1	6	0	-2.074992	0.689055	0.803667
2	6	0	-0.784231	1.468138	0.871470
3	6	0	0.409884	0.790579	0.174358
4	6	0	-2.846073	0.701067	-0.296560
5	8	0	-2.409099	-0.055833	1.894481
6	8	0	1.488178	1.715839	0.154877
7	6	0	2.218810	1.828767	-2.171249
8	6	0	1.556854	2.536608	-0.997504
9	1	0	-0.517900	1.701935	1.907945
10	1	0	-0.926250	2.427558	0.364081
11	1	0	0.098956	0.548664	-0.851530
12	1	0	-2.495608	1.343599	-1.101664
13	1	0	2.373033	2.527884	-2.999071
14	1	0	1.609015	0.998008	-2.538423
15	1	0	3.186707	1.422855	-1.862433

16	1	0	2.144190	3.410381	-0.700769
17	1	0	0.553538	2.895484	-1.276349
18	6	0	-4.096546	-0.015528	-0.566257
19	6	0	-4.763504	0.253741	-1.772281
20	6	0	-4.667044	-0.961487	0.302212
21	6	0	-5.951428	-0.386024	-2.102490
22	1	0	-4.337226	0.981587	-2.458924
23	6	0	-5.855647	-1.600857	-0.032043
24	1	0	-4.174929	-1.194154	1.237197
25	6	0	-6.506041	-1.319988	-1.231014
26	1	0	-6.444754	-0.155545	-3.042317
27	1	0	-6.277289	-2.329023	0.654959
28	1	0	-7.433843	-1.823919	-1.483952
29	6	0	4.029720	-2.227992	-1.666156
30	6	0	4.304835	-1.832820	-0.372957
31	6	0	3.294585	-1.283336	0.440426
32	6	0	1.980349	-1.134766	-0.069861
33	6	0	1.723780	-1.541264	-1.388772
34	6	0	2.727936	-2.084152	-2.170660
35	1	0	4.625019	-0.972648	2.123579
36	1	0	4.810341	-2.655048	-2.287037
37	1	0	5.306409	-1.944308	0.035212
38	6	0	3.595232	-0.864740	1.788523
39	6	0	0.965008	-0.516723	0.783182
40	1	0	0.714867	-1.450089	-1.782804
41	1	0	2.504242	-2.409295	-3.182401
42	6	0	1.320034	-0.406170	2.175703
43	6	0	2.653317	-0.415892	2.665603
44	1	0	-0.148137	-0.823566	1.707834
45	1	0	2.870168	-0.196373	3.704659
46	8	0	0.231096	-0.454230	2.876135
47	1	0	-1.757996	0.085262	2.599222

Optimized Cartesian coordinates for **ts-i23**

Center Number	Atomic Number	Atomic Type	Coordinates (Angstroms) X	Y	Z
1	6	0	-2.140976	0.847990	0.277730
2	6	0	-1.095121	1.697211	-0.304562
3	6	0	0.332815	1.439551	-0.179175
4	6	0	-3.268906	0.526274	-0.395052
5	8	0	-1.957630	0.412246	1.556388
6	8	0	0.682807	2.803855	0.760774
7	6	0	3.008245	3.222838	0.328490
8	6	0	1.593235	3.752435	0.195042
9	1	0	-0.433488	2.882677	0.533206
10	1	0	-1.368565	2.111271	-1.272836
11	1	0	0.899003	1.722061	-1.069663
12	1	0	-3.307152	0.863820	-1.426981
13	1	0	3.727688	3.951589	-0.055184
14	1	0	3.130417	2.289464	-0.229735
15	1	0	3.232031	3.021673	1.379151
16	1	0	1.462717	4.685317	0.749744
17	1	0	1.324972	3.933046	-0.856185
18	6	0	-4.456216	-0.190340	0.066225
19	6	0	-5.546957	-0.286451	-0.817139
20	6	0	-4.592919	-0.798975	1.328027
21	6	0	-6.717426	-0.945598	-0.466391
22	1	0	-5.463847	0.172263	-1.799920
23	6	0	-5.768001	-1.455910	1.677056
24	1	0	-3.770430	-0.756904	2.029219
25	6	0	-6.837932	-1.536618	0.789289
26	1	0	-7.538469	-0.998812	-1.176131
27	1	0	-5.846007	-1.916500	2.658480
28	1	0	-7.749602	-2.055591	1.069482

29	6	0	2.621322	-2.768210	-2.047880
30	6	0	2.767983	-2.851717	-0.688353
31	6	0	2.211413	-1.867010	0.166927
32	6	0	1.506848	-0.761670	-0.388829
33	6	0	1.347767	-0.721937	-1.802174
34	6	0	1.890502	-1.694339	-2.604223
35	1	0	2.869629	-2.812532	2.000755
36	1	0	3.045657	-3.527972	-2.696125
37	1	0	3.306208	-3.681673	-0.237723
38	6	0	2.331919	-1.969912	1.575292
39	6	0	0.964763	0.249052	0.473426
40	1	0	0.748839	0.060180	-2.256495
41	1	0	1.743752	-1.645154	-3.678778
42	6	0	1.071836	0.072925	1.837323
43	6	0	1.764588	-1.031373	2.388632
44	1	0	0.577564	0.670397	3.590849
45	1	0	1.841535	-1.116951	3.470337
46	8	0	0.511416	0.995582	2.681096
47	1	0	-1.252933	0.931627	1.977357

Optimized Cartesian coordinates for **ts-II**

Center Number	Atomic Number	Atomic Type	Coordinates (Angstroms) X	Y	Z
1	6	0	-2.664506	-0.392017	2.001631
2	6	0	-3.659633	-1.426754	1.751151
3	6	0	-3.684939	-2.417422	0.825184
4	6	0	-1.437412	0.060202	1.384095
5	8	0	-2.871412	0.377776	3.016288
6	1	0	-4.455201	-1.415605	2.491959
7	1	0	-4.486670	-3.143487	0.963867
8	1	0	-1.619188	1.033559	0.916104
9	6	0	-0.404656	-0.741673	0.723019
10	6	0	0.395442	-0.169328	-0.276490
11	6	0	-0.167491	-2.079824	1.068779
12	6	0	1.389036	-0.905862	-0.910450
13	1	0	0.223166	0.866058	-0.560771
14	6	0	0.804277	-2.827354	0.414116
15	1	0	-0.773387	-2.543515	1.845265
16	6	0	1.591689	-2.243241	-0.576678
17	1	0	1.996899	-0.438353	-1.679926
18	1	0	0.942705	-3.872655	0.676975
19	1	0	2.356750	-2.824956	-1.081824
20	6	0	-1.324316	-6.656281	-0.883565
21	6	0	-1.034981	-5.669043	-1.793986
22	6	0	-1.526838	-4.354495	-1.622410
23	6	0	-2.339997	-4.047287	-0.499822
24	6	0	-2.599509	-5.078413	0.437230
25	6	0	-2.112266	-6.350703	0.245088
26	1	0	-0.566477	-3.552921	-3.391281
27	1	0	-0.939880	-7.661640	-1.021402
28	1	0	-0.415109	-5.881936	-2.661344
29	6	0	-1.199137	-3.315947	-2.540000
30	6	0	-2.810512	-2.700740	-0.307472
31	1	0	-3.169398	-4.858543	1.334706
32	1	0	-2.325309	-7.123418	0.977556
33	6	0	-2.469653	-1.731148	-1.239859
34	6	0	-1.659408	-2.046693	-2.361412
35	1	0	-3.427391	-0.320453	-0.390977
36	1	0	-1.415693	-1.241011	-3.044983
37	8	0	-2.892378	-0.452357	-1.189893
38	1	0	-1.697891	0.721378	2.679030

Optimized Cartesian coordinates for **ts-i45**

Center Number	Atomic Number	Atomic Type	Coordinates (Angstroms) X	Y	Z
1	6	0	2.311432	1.810950	-1.428350
2	6	0	1.024132	1.754753	-0.854829
3	6	0	0.705059	1.061103	0.287586
4	6	0	3.640696	1.776181	-0.719537
5	8	0	2.420361	2.204770	-2.692601
6	1	0	0.234057	2.101942	-1.511894
7	1	0	1.530444	0.596047	0.815695
8	1	0	4.388765	1.609017	-1.499392
9	6	0	3.783479	0.753920	0.381839
10	6	0	3.745391	-0.602380	0.047992
11	6	0	3.901179	1.128516	1.719171
12	6	0	3.788628	-1.569307	1.047376
13	1	0	3.637304	-0.873139	-0.999378
14	6	0	3.948476	0.159341	2.719745
15	1	0	3.930712	2.183179	1.982307
16	6	0	3.882645	-1.190073	2.386627
17	1	0	3.743116	-2.622279	0.782859
18	1	0	4.025358	0.460745	3.759740
19	1	0	3.903935	-1.944771	3.166466
20	6	0	-4.188890	3.014703	0.369639
21	6	0	-4.192444	1.826750	1.060596
22	6	0	-3.000565	1.092069	1.251173
23	6	0	-1.779168	1.561934	0.693586
24	6	0	-1.796722	2.819071	0.043105
25	6	0	-2.970560	3.521361	-0.121585
26	1	0	-3.953755	-0.465380	2.415626
27	1	0	-5.109358	3.570959	0.224847
28	1	0	-5.114739	1.434007	1.481304
29	6	0	-3.009548	-0.115529	2.006360
30	6	0	-0.579374	0.775518	0.865326
31	1	0	-0.869452	3.261718	-0.297474
32	1	0	-2.951105	4.482806	-0.625812
33	6	0	-0.657219	-0.411900	1.607453
34	6	0	-1.869075	-0.836481	2.199599
35	1	0	0.953346	-1.294980	1.006339
36	1	0	-1.862247	-1.773990	2.743608
37	8	0	0.400067	-1.232602	1.807048
38	1	0	3.812386	2.787198	-0.323800
39	6	0	-3.466485	-2.853228	-0.214633
40	6	0	-2.164419	-3.289350	-0.186975
41	6	0	-1.137830	-2.549673	-0.822058
42	6	0	-1.463746	-1.347171	-1.521256
43	6	0	-2.822713	-0.918693	-1.521504
44	6	0	-3.793282	-1.650178	-0.888344
45	1	0	0.480706	-3.882338	-0.280956
46	1	0	-4.246941	-3.424542	0.278864
47	1	0	-1.898728	-4.206114	0.334657
48	6	0	0.226580	-2.955505	-0.791790
49	6	0	-0.444678	-0.597087	-2.134705
50	1	0	-3.073380	0.012054	-2.025531
51	1	0	-4.822194	-1.300884	-0.893059
52	6	0	0.912261	-0.961824	-2.075722
53	6	0	1.207506	-2.199216	-1.374698
54	1	0	-0.710305	0.311118	-2.671471
55	1	0	2.239682	-2.537418	-1.370156
56	8	0	1.858246	-0.231321	-2.553189
57	1	0	1.864094	1.548909	-3.183639

Optimized Cartesian coordinates for **ts-i5III**

Center Number	Atomic Number	Atomic Type	Coordinates (Angstroms) X	Y	Z

1	6	0	1.739891	-6.229903	2.166874
2	6	0	0.794817	-5.967415	1.170545
3	6	0	0.297824	-4.687776	0.962442
4	6	0	2.833783	-5.289488	2.623074
5	8	0	2.028500	-7.496630	2.500303
6	1	0	0.357464	-6.825067	0.667273
7	1	0	0.846064	-3.891448	1.460083
8	1	0	2.519002	-4.814245	3.555279
9	6	0	3.285974	-4.241458	1.629093
10	6	0	3.361055	-2.898489	2.004923
11	6	0	3.651731	-4.594634	0.325371
12	6	0	3.794518	-1.927092	1.101591
13	1	0	3.055782	-2.610083	3.007390
14	6	0	4.081208	-3.628455	-0.578563
15	1	0	3.580782	-5.634383	0.015971
16	6	0	4.155088	-2.289936	-0.192699
17	1	0	3.832815	-0.886300	1.407184
18	1	0	4.352653	-3.918270	-1.588895
19	1	0	4.478616	-1.534829	-0.901816
20	6	0	-4.048858	-6.139355	-1.650970
21	6	0	-3.643106	-4.931313	-2.158786
22	6	0	-2.482378	-4.283927	-1.671177
23	6	0	-1.698877	-4.895035	-0.649820
24	6	0	-2.159887	-6.136083	-0.133473
25	6	0	-3.297701	-6.737794	-0.618379
26	1	0	-2.719783	-2.548085	-2.942813
27	1	0	-4.942641	-6.625625	-2.028168
28	1	0	-4.213872	-4.440550	-2.943302
29	6	0	-2.109296	-3.005633	-2.168626
30	6	0	-0.536048	-4.212900	-0.146666
31	1	0	-1.623428	-6.612567	0.676784
32	1	0	-3.624072	-7.683001	-0.194862
33	6	0	-0.213063	-2.969798	-0.683312
34	6	0	-1.009765	-2.362901	-1.686502
35	1	0	1.524954	-2.771027	0.152890
36	1	0	-0.699259	-1.390201	-2.051841
37	8	0	0.867845	-2.238650	-0.323213
38	1	0	3.679483	-5.938109	2.881413
39	6	0	-2.585584	-0.569086	1.834804
40	6	0	-1.506498	-0.749279	2.673799
41	6	0	-1.066690	-2.044619	3.013239
42	6	0	-1.748211	-3.172229	2.488537
43	6	0	-2.866313	-2.963352	1.649753
44	6	0	-3.271638	-1.687065	1.323584
45	1	0	0.511149	-1.391872	4.354780
46	1	0	-2.909910	0.432653	1.570880
47	1	0	-0.977166	0.108313	3.082300
48	6	0	0.035695	-2.263899	3.909298
49	6	0	-1.228705	-4.480194	2.741210
50	1	0	-3.392721	-3.827629	1.252088
51	1	0	-4.123182	-1.543460	0.665013
52	6	0	-0.153326	-4.701260	3.645183
53	6	0	0.463829	-3.514349	4.225312
54	1	0	-1.802406	-5.344038	2.422217
55	1	0	1.260880	-3.670850	4.947884
56	8	0	0.348726	-5.854556	3.814137
57	1	0	1.229125	-8.036005	2.395386

Optimized Cartesian coordinates for **ts-III**

Center Number	Atomic Number	Atomic Type	Coordinates (Angstroms) X	Y	Z
1	6	0	1.004318	1.932008	-0.900491
2	6	0	-0.035091	1.591235	-0.132289
3	6	0	-0.795776	0.285331	-0.262704

4	6	0	1.626691	1.105578	-1.987924
5	8	0	1.669571	3.119413	-0.758269
6	1	0	-0.362194	2.308003	0.617319
7	1	0	-1.183969	0.274172	-1.292231
8	1	0	0.878192	0.427875	-2.412088
9	6	0	2.829934	0.292606	-1.534861
10	6	0	3.207505	-0.826016	-2.278131
11	6	0	3.571662	0.625732	-0.398147
12	6	0	4.304165	-1.596893	-1.902056
13	1	0	2.622876	-1.106914	-3.151660
14	6	0	4.660883	-0.150393	-0.013623
15	1	0	3.288607	1.490577	0.194093
16	6	0	5.033274	-1.262931	-0.764678
17	1	0	4.578393	-2.467463	-2.491150
18	1	0	5.213935	0.110393	0.883916
19	1	0	5.883293	-1.867402	-0.461918
20	6	0	3.005444	-1.510544	2.903081
21	6	0	2.902933	-2.408561	1.872757
22	6	0	1.922339	-2.251306	0.861504
23	6	0	1.037013	-1.135770	0.900285
24	6	0	1.152942	-0.238864	1.997950
25	6	0	2.109687	-0.419440	2.965871
26	1	0	2.492719	-4.038164	-0.217427
27	1	0	3.761082	-1.637662	3.672031
28	1	0	3.576631	-3.259629	1.809703
29	6	0	1.808917	-3.193661	-0.193389
30	6	0	0.083197	-0.951037	-0.150645
31	1	0	0.469883	0.598262	2.073929
32	1	0	2.173448	0.280103	3.794230
33	6	0	-0.016413	-1.929502	-1.124138
34	6	0	0.848815	-3.049220	-1.152511
35	1	0	-1.777112	-1.558503	-1.803441
36	1	0	0.720716	-3.766780	-1.955980
37	8	0	-0.927389	-1.877430	-2.147826
38	1	0	1.932963	1.793824	-2.785901
39	6	0	-4.428425	-3.266536	-0.401464
40	6	0	-4.868966	-1.996723	-0.717100
41	6	0	-4.116213	-0.863549	-0.350585
42	6	0	-2.884817	-1.021061	0.344690
43	6	0	-2.471251	-2.325037	0.675889
44	6	0	-3.229809	-3.424295	0.308721
45	1	0	-5.531109	0.524772	-1.237452
46	1	0	-5.013310	-4.135323	-0.684770
47	1	0	-5.809521	-1.855553	-1.243912
48	6	0	-4.608991	0.460943	-0.663328
49	6	0	-2.092579	0.180946	0.643885
50	1	0	-1.557292	-2.458175	1.244827
51	1	0	-2.894216	-4.419178	0.584935
52	6	0	-2.878804	1.399628	0.622271
53	6	0	-4.026195	1.600707	-0.199322
54	1	0	-1.779381	1.140948	1.775158
55	1	0	-4.455810	2.585747	-0.341327
56	8	0	-2.419223	2.192148	1.522475
57	1	0	1.268122	3.618276	-0.030570

Optimized Cartesian coordinates for **ts-IIIi6**

Center Number	Atomic Number	Atomic Type	Coordinates (Angstroms) X	Y	Z
1	6	0	-0.859714	-2.766253	-0.575227
2	6	0	0.398225	-2.096668	-0.304068
3	6	0	0.380605	-0.614623	0.123668
4	6	0	-2.213541	-2.159024	-0.604083
5	8	0	-0.849261	-4.045328	-0.804944
6	1	0	1.050217	-2.719885	0.319812

7	1	0	-0.350290	-0.537442	0.934682
8	1	0	-2.190855	-1.353823	-1.349238
9	6	0	-2.530944	-1.570468	0.760538
10	6	0	-2.956389	-0.246605	0.868594
11	6	0	-2.306040	-2.320135	1.918734
12	6	0	-3.139505	0.327825	2.123825
13	1	0	-3.094324	0.350691	-0.028843
14	6	0	-2.485160	-1.744140	3.174300
15	1	0	-1.981627	-3.356594	1.840767
16	6	0	-2.895732	-0.415215	3.276884
17	1	0	-3.440865	1.367965	2.193192
18	1	0	-2.295762	-2.327945	4.069638
19	1	0	-3.019897	0.039710	4.254297
20	6	0	5.287945	0.215341	-1.599300
21	6	0	5.325389	0.383762	-0.239545
22	6	0	4.157183	0.226310	0.546664
23	6	0	2.916278	-0.100150	-0.074209
24	6	0	2.914160	-0.274257	-1.486185
25	6	0	4.066399	-0.123412	-2.219667
26	1	0	5.158513	0.632193	2.423487
27	1	0	6.187497	0.336551	-2.194909
28	1	0	6.254897	0.637593	0.264348
29	6	0	4.210190	0.377444	1.957401
30	6	0	1.735740	-0.258066	0.729231
31	1	0	2.003100	-0.538852	-2.008977
32	1	0	4.030303	-0.264551	-3.295703
33	6	0	1.858525	-0.135508	2.103569
34	6	0	3.094059	0.196316	2.716787
35	1	0	0.017765	-0.562368	2.580193
36	1	0	3.106596	0.296844	3.796870
37	8	0	0.842207	-0.284864	3.005671
38	1	0	-2.933942	-2.921713	-0.914385
39	6	0	-1.604285	4.184021	0.141624
40	6	0	-1.720827	3.736667	-1.152360
41	6	0	-1.246215	2.461990	-1.535381
42	6	0	-0.618305	1.608025	-0.578153
43	6	0	-0.515094	2.105262	0.754274
44	6	0	-0.995341	3.347308	1.099410
45	1	0	-1.884171	2.644998	-3.597372
46	1	0	-1.971372	5.165209	0.425328
47	1	0	-2.188772	4.359346	-1.911953
48	6	0	-1.406876	1.991141	-2.870117
49	6	0	-0.171115	0.306368	-0.963883
50	1	0	-0.052177	1.504016	1.528768
51	1	0	-0.893926	3.689347	2.125809
52	6	0	-0.333468	-0.145406	-2.297157
53	6	0	-0.974165	0.754187	-3.230835
54	1	0	0.759966	-2.058887	-1.384849
55	1	0	-1.088045	0.378964	-4.243460
56	8	0	0.029441	-1.312658	-2.723589
57	1	0	0.063365	-4.394596	-0.796016

Optimized Cartesian coordinates for **ts-i67**

Center Number	Atomic Number	Atomic Type	Coordinates (Angstroms) X	Y	Z
1	6	0	-2.601248	-0.368651	-1.221558
2	6	0	-1.239188	-0.671664	-1.781447
3	6	0	-0.348743	-0.288922	-0.628898
4	6	0	-3.145736	-0.362154	0.233972
5	8	0	-3.390273	-1.615299	-1.760327
6	1	0	-1.098794	-1.689418	-2.106019
7	1	0	-0.874025	-0.588588	0.282717
8	1	0	-2.626177	0.447449	0.751975
9	6	0	-3.193149	-1.592467	1.107795

10	6	0	-2.284027	-1.746862	2.155804
11	6	0	-4.190930	-2.553197	0.936860
12	6	0	-2.339108	-2.858260	2.985652
13	1	0	-1.516234	-0.993445	2.317037
14	6	0	-4.245566	-3.672840	1.763211
15	1	0	-4.936366	-2.423837	0.155394
16	6	0	-3.315868	-3.831151	2.785015
17	1	0	-1.615805	-2.968349	3.787351
18	1	0	-5.022799	-4.416069	1.613445
19	1	0	-3.357040	-4.703535	3.429693
20	6	0	4.910162	-1.213698	-1.323436
21	6	0	4.308558	-2.396859	-0.974789
22	6	0	2.910755	-2.478847	-0.761560
23	6	0	2.110352	-1.299784	-0.871468
24	6	0	2.760697	-0.097635	-1.278206
25	6	0	4.114843	-0.056215	-1.493796
26	1	0	2.882229	-4.606193	-0.380612
27	1	0	5.981854	-1.166964	-1.489507
28	1	0	4.897805	-3.305508	-0.869418
29	6	0	2.268687	-3.712458	-0.475693
30	6	0	0.719551	-1.382502	-0.627457
31	1	0	2.161821	0.792700	-1.445273
32	1	0	4.578804	0.873809	-1.810440
33	6	0	0.058862	-2.647735	-0.478355
34	6	0	0.909717	-3.797147	-0.364166
35	1	0	-2.690891	-2.290765	-1.280668
36	1	0	0.414050	-4.748117	-0.192757
37	8	0	-1.245522	-2.815329	-0.446501
38	1	0	-4.168698	0.001055	0.071639
39	6	0	1.923478	4.052009	1.359460
40	6	0	0.859161	4.496530	0.620154
41	6	0	0.001878	3.579317	-0.042514
42	6	0	0.285211	2.185264	0.027986
43	6	0	1.383171	1.754261	0.822706
44	6	0	2.175891	2.663989	1.473635
45	1	0	-1.366990	5.078365	-0.795985
46	1	0	2.568502	4.760530	1.869737
47	1	0	0.641651	5.558646	0.542557
48	6	0	-1.155290	4.014648	-0.735072
49	6	0	-0.546402	1.239035	-0.644227
50	1	0	1.581464	0.690776	0.912887
51	1	0	3.006481	2.316446	2.079777
52	6	0	-1.744674	1.729571	-1.200879
53	6	0	-2.029005	3.107453	-1.270027
54	1	0	-1.067924	-0.015305	-2.639130
55	1	0	-2.956136	3.413459	-1.742695
56	8	0	-2.847317	0.930059	-1.678718
57	1	0	-3.241816	-1.709171	-2.723946

Optimized Cartesian coordinates for **ts-i78**

Center Number	Atomic Number	Atomic Type	Coordinates (Angstroms) X	Y	Z
1	6	0	-1.229795	-1.231897	0.776226
2	6	0	-0.321888	-0.620371	1.793552
3	6	0	0.481230	0.029557	0.655469
4	6	0	-1.511161	-1.529287	-0.767510
5	8	0	-3.101768	-3.251547	1.291551
6	1	0	-0.812394	0.088752	2.440359
7	1	0	0.104799	-0.235917	-0.324775
8	1	0	-0.589411	-1.475227	-1.354976
9	6	0	-2.646269	-0.767721	-1.404508
10	6	0	-2.449689	0.438506	-2.063757
11	6	0	-3.942386	-1.290058	-1.298201
12	6	0	-3.537270	1.161152	-2.550234

13	1	0	-1.447698	0.860374	-2.133322
14	6	0	-5.030955	-0.585954	-1.803203
15	1	0	-4.084675	-2.255511	-0.800804
16	6	0	-4.827245	0.648967	-2.419276
17	1	0	-3.376293	2.123325	-3.027333
18	1	0	-6.033433	-0.993132	-1.712584
19	1	0	-5.675311	1.210340	-2.800925
20	6	0	0.625067	5.446817	-0.036508
21	6	0	-0.688810	5.061318	-0.011778
22	6	0	-1.056398	3.708956	0.211050
23	6	0	-0.039592	2.721480	0.395947
24	6	0	1.310821	3.165282	0.381053
25	6	0	1.635190	4.480762	0.173251
26	1	0	-3.183592	4.061384	0.035732
27	1	0	0.891723	6.484933	-0.206863
28	1	0	-1.481600	5.790454	-0.158262
29	6	0	-2.416385	3.317973	0.233763
30	6	0	-0.399579	1.360978	0.621365
31	1	0	2.098019	2.451638	0.564411
32	1	0	2.678135	4.782475	0.175273
33	6	0	-1.776805	1.031757	0.723601
34	6	0	-2.761653	2.020814	0.479037
35	1	0	-3.408524	-2.391132	1.644404
36	1	0	-3.789250	1.679908	0.412339
37	8	0	-2.362754	-0.197400	1.054265
38	1	0	-1.767453	-2.587973	-0.747658
39	6	0	5.730268	-0.815310	-0.394210
40	6	0	5.158141	-2.046691	-0.208392
41	6	0	3.776011	-2.179461	0.086802
42	6	0	2.975390	-1.004052	0.201888
43	6	0	3.599824	0.251136	-0.004820
44	6	0	4.933746	0.351445	-0.295245
45	1	0	3.775704	-4.339766	0.197602
46	1	0	6.788485	-0.729964	-0.619613
47	1	0	5.756381	-2.951126	-0.286502
48	6	0	3.167634	-3.442402	0.274805
49	6	0	1.599399	-1.105575	0.523239
50	1	0	2.961833	1.116654	0.066761
51	1	0	5.383796	1.327268	-0.450392
52	6	0	1.002171	-2.393811	0.646541
53	6	0	1.830063	-3.541690	0.545328
54	1	0	0.240073	-1.309648	2.408730
55	1	0	1.348737	-4.504271	0.681230
56	8	0	-0.326691	-2.686042	0.887452
57	1	0	-2.457370	-3.563974	1.936308

Optimized Cartesian coordinates for **ts-IIin1**

Center Number	Atomic Number	Atomic Type	Coordinates (Angstroms) X	Y	Z
1	6	0	-2.332864	-1.324436	-0.132219
2	6	0	-1.234106	-1.007132	-0.961815
3	6	0	-0.239362	-0.198666	-0.428387
4	6	0	-3.368654	-0.393286	0.431748
5	8	0	-2.396489	-2.562662	0.210567
6	1	0	-0.858491	-1.882629	-1.481980
7	1	0	-0.441024	0.798043	-0.031770
8	1	0	-4.305527	-0.655441	-0.081962
9	6	0	-3.044228	1.067007	0.246131
10	6	0	-3.063797	1.640910	-1.027120
11	6	0	-2.658119	1.847498	1.336641
12	6	0	-2.686322	2.967636	-1.207786
13	1	0	-3.359071	1.037749	-1.881715
14	6	0	-2.284319	3.177113	1.159292
15	1	0	-2.637736	1.406185	2.330104

16	6	0	-2.291968	3.737627	-0.115077
17	1	0	-2.700297	3.401314	-2.202950
18	1	0	-1.984174	3.772323	2.015990
19	1	0	-1.997156	4.772713	-0.257101
20	6	0	4.640521	1.466053	-0.114208
21	6	0	4.655847	0.118073	0.176837
22	6	0	3.471635	-0.641637	0.141610
23	6	0	2.243086	-0.028485	-0.201095
24	6	0	2.259013	1.344693	-0.529708
25	6	0	3.427582	2.077739	-0.469737
26	1	0	4.427390	-2.514840	0.681982
27	1	0	5.556780	2.046652	-0.084460
28	1	0	5.586482	-0.379855	0.438438
29	6	0	3.476230	-2.047975	0.434041
30	6	0	1.025442	-0.812331	-0.244547
31	1	0	1.342310	1.829535	-0.853543
32	1	0	3.409569	3.134885	-0.717970
33	6	0	1.042948	-2.214355	0.125310
34	6	0	2.343414	-2.788206	0.420733
35	1	0	-1.320750	-2.873401	0.186478
36	1	0	2.347237	-3.844058	0.669671
37	8	0	0.036694	-2.981161	0.332375
38	1	0	-3.517346	-0.647753	1.485794

Optimized Cartesian coordinates for **ts-in12**

Center Number	Atomic Number	Atomic Type	Coordinates (Angstroms) X	Y	Z
1	6	0	-1.872033	-1.633636	-0.548330
2	6	0	-0.909575	-1.225839	-1.521094
3	6	0	-0.108435	-0.143034	-1.195988
4	6	0	-2.836189	-0.756025	0.229850
5	8	0	-2.356837	-2.878223	-0.759115
6	1	0	-0.337682	-2.118284	-1.778355
7	1	0	-0.452143	0.889221	-1.140426
8	1	0	-3.753702	-0.723442	-0.370384
9	6	0	-2.381597	0.641395	0.557030
10	6	0	-2.796888	1.716962	-0.229297
11	6	0	-1.506131	0.873536	1.620931
12	6	0	-2.314742	3.000104	0.016255
13	1	0	-3.486368	1.543021	-1.052055
14	6	0	-1.019928	2.153039	1.864804
15	1	0	-1.187460	0.037938	2.238426
16	6	0	-1.416715	3.218143	1.057936
17	1	0	-2.637437	3.828241	-0.607422
18	1	0	-0.323846	2.318230	2.681335
19	1	0	-1.031716	4.215835	1.244941
20	6	0	4.765887	1.400494	-0.072052
21	6	0	4.350648	0.544034	0.922875
22	6	0	3.100169	-0.104073	0.839249
23	6	0	2.269169	0.116291	-0.285952
24	6	0	2.718796	0.993810	-1.297684
25	6	0	3.936620	1.628750	-1.188028
26	1	0	3.253465	-1.131268	2.743155
27	1	0	5.728833	1.896187	-0.001325
28	1	0	4.978980	0.357838	1.790710
29	6	0	2.621358	-0.967741	1.872838
30	6	0	1.008961	-0.556173	-0.399670
31	1	0	2.091748	1.143341	-2.172911
32	1	0	4.266588	2.302424	-1.973288
33	6	0	0.548774	-1.428315	0.648884
34	6	0	1.401971	-1.564554	1.804869
35	1	0	-2.780728	-3.193603	0.054191
36	1	0	1.040009	-2.200512	2.605553
37	8	0	-0.613922	-2.016703	0.727594

38	1	0	-3.071932	-1.299993	1.153290

Optimized Cartesian coordinates for **ts-in33**

Center Number	Atomic Number	Atomic Type	Coordinates (Angstroms) X	Y	Z
1	6	0	-1.749455	-0.083668	1.285055
2	6	0	-0.558249	-0.766270	1.487855
3	6	0	0.698750	-0.311689	0.748318
4	6	0	-3.060439	-0.518751	1.868383
5	1	0	-0.442382	-1.308647	2.425299
6	1	0	1.559011	-0.324427	1.419620
7	1	0	-2.969070	-1.576292	2.141436
8	6	0	-4.280705	-0.296865	0.994865
9	6	0	-4.234223	-0.484840	-0.388189
10	6	0	-5.488031	0.059051	1.596394
11	6	0	-5.388503	-0.320123	-1.148565
12	1	0	-3.292811	-0.735321	-0.872963
13	6	0	-6.641912	0.217445	0.834389
14	1	0	-5.526312	0.214367	2.672399
15	6	0	-6.593826	0.027127	-0.543284
16	1	0	-5.341675	-0.460456	-2.224342
17	1	0	-7.574218	0.494782	1.317193
18	1	0	-7.490137	0.155059	-1.142896
19	6	0	3.827476	3.239576	-1.452961
20	6	0	2.579012	3.805862	-1.421496
21	6	0	1.470395	3.097396	-0.893458
22	6	0	1.662582	1.783000	-0.379961
23	6	0	2.964052	1.217120	-0.441526
24	6	0	4.016653	1.927624	-0.961867
25	1	0	0.028000	4.667141	-1.279039
26	1	0	4.668970	3.789619	-1.862428
27	1	0	2.416811	4.809191	-1.807201
28	6	0	0.168650	3.667856	-0.876849
29	6	0	0.553021	1.070726	0.167123
30	1	0	3.124218	0.199977	-0.096362
31	1	0	5.002330	1.474570	-1.006603
32	6	0	-0.677134	1.675142	0.145845
33	6	0	-0.891789	2.969794	-0.373526
34	1	0	-1.899280	3.370911	-0.358909
35	8	0	-1.816342	1.076432	0.650922
36	1	0	-3.196506	0.035514	2.807989
37	6	0	3.918621	-4.372463	-0.366469
38	6	0	2.886546	-4.406688	-1.284959
39	6	0	1.859341	-3.450703	-1.260843
40	6	0	1.861584	-2.425368	-0.277938
41	6	0	2.926232	-2.414349	0.648336
42	6	0	3.932571	-3.363472	0.603349
43	1	0	0.834623	-4.287934	-2.983637
44	1	0	4.708895	-5.115505	-0.398057
45	1	0	2.856687	-5.179731	-2.049361
46	6	0	0.801893	-3.490797	-2.243586
47	6	0	0.759355	-1.476427	-0.246814
48	1	0	2.972252	-1.653121	1.420346
49	1	0	4.737690	-3.321621	1.330905
50	6	0	-0.249910	-1.476481	-1.305447
51	6	0	-0.193398	-2.581984	-2.264061
52	1	0	-0.409959	-1.835475	0.665892
53	1	0	-0.979075	-2.601412	-3.013035
54	8	0	-1.180634	-0.652606	-1.323810

Table S1. Calculated relative energies (all in kcal mol^{-1}, relative to isolated species) for the ZPE-corrected Gibbs free energies (ΔG_{gas}), Gibbs free energies for all species in solution phase (ΔG_{sol}) at 298 K by M06-2X/6-311++G(d,p)//M06-2X/6-31G(d) method and difference between absolute energy.

Species	ΔG_{gas}	$\Delta G_{sol(toluene)}$
1+2	0.00	0.00
i0	0.71	-2.61
ts-i01	20.58	13.04
i1	5.16	1.56
ts-i1I	34.39	28.34
I	-11.63	-17.51
ts-Ii2	16.65	7.99
i2	-5.37	-8.97
ts-i23	13.34	7.31
i3	-15.59	-18.10
1+2-etoh	0.00	0.00
II-0	2.27	-2.83
ts-II	24.74	18.88
II	-8.53	-14.06
ts-IIin1	3.29	-3.88
in1	-10.04	-16.11
ts-in12	10.44	2.05
in2	-15.97	-22.36
1+2*2-etoh-h2o	0.00	0.00
in3	-16.08	-12.05
ts-in33	9.87	11.25
3	-30.83	-36.79
1+2*2-etoh	0.00	0.00
i4	-17.26	-26.91
ts-i45	0.98	-11.40
i5	-10.78	-21.48
ts-i5III	-1.19	-14.85
III-0	-18.47	-25.03
ts-III	8.24	-1.56
III	-22.92	-29.44
ts-IIIi6	-10.65	-20.19
i6	-33.98	-36.68
ts-i67	-3.22	-9.45
i7	-28.71	-33.67
ts-i78	2.41	-4.24
i8	-17.78	-19.29
in4+h	0.0	0.0
ts-in45+h	10.2	7.8
in5+h	-2.9	-7.2
ts-in53+h	-0.5	-3.9
3+h	-15.5	-20.7

Table S2. The activation energy (local barrier) (in kcal mol^{-1}) of all reactions in the gas, solution phase calculated with M06-2X/6-311++G(d,p)//M06-2X/6-31G(d) method.

TS	$\Delta G^{\neq}_{gas}$	$\Delta G^{\neq}_{sol}$
ts-i01 (1746i)	19.9	15.7
ts-i1I (564i)	29.2	26.8
ts-Ii2 (2203i)	28.3	25.5
ts-i23 (1533i)	18.7	16.3
ts-II (2227i)	22.5	21.7
ts-i45 (108i)	18.2	15.5
ts-i5III (309i)	9.6	6.7
ts-III (2132i)	26.7	23.4
ts-IIIi6 (760i)	12.3	9.2
ts-i67 (383i)	30.8	27.3
ts-i78 (263i)	31.1	29.5
ts-IIin1 (869i)	11.8	10.2
ts-in12 (379i)	20.5	18.1
ts-in33 (1500i)	26.0	23.3
ts-in45h+ (1502i)	10.2	7.8

ts-in53h+ (86i)	2.4	3.3

Table S3. Mayer bond order (MBO) of typical TSs

	O1···H1	H1···O2	O1···C4	
ts-i01	0.36	0.35	0.45	
	C1···C2	C2···C5		
ts-i1I	0.35	0.17		
	C1···H2	H2···O1		
ts-Ii2	0.38	0.35		
	C2···O3	C3···H3	C2···C3	O3···H3
ts-i23	0.53	0.38	1.19	0.43
	O2···H1	C5···H1		
ts-II	0.36	0.41		
	O1···H2	H2···O2		
ts-IIin1	0.26	0.44		
	O1···C4			
ts-in12	0.46			
	C6···H5	C3···H5	O4···C4	
ts-in33	0.36	0.47	0.16	
	O4···H4	H4···O2	O4···C4	
ts-i45	0.13	0.65	0.16	
	O4···C4	C6···C2		
ts-i5III	0.24	0.28		
	C6···H5	H5···O4		
ts-III	0.41	0.38		
	O4···H5	H5···C3	C4···O4	
ts-IIIi6	0.16	0.68	0.18	
	O1···H2	H2···O2	O2···C4	
ts-i67	0.22	0.48	0.60	
	O1···C4			
ts-i78	0.76			

Figure S1. Evolution of bond lengths along the IRC for (a) **ts-i01** (b) **ts-i23** (c) **ts-i5III** (d) **ts-i67** (e) **ts-IIin1** (f) **ts-in33** at M06-2X/6-311++G(d,p) level.

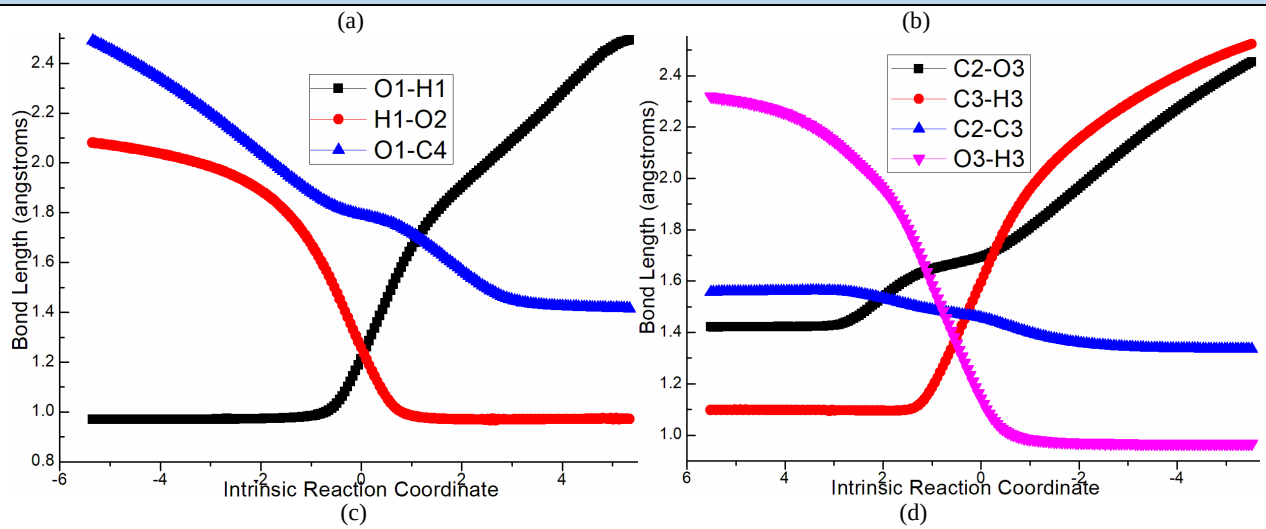

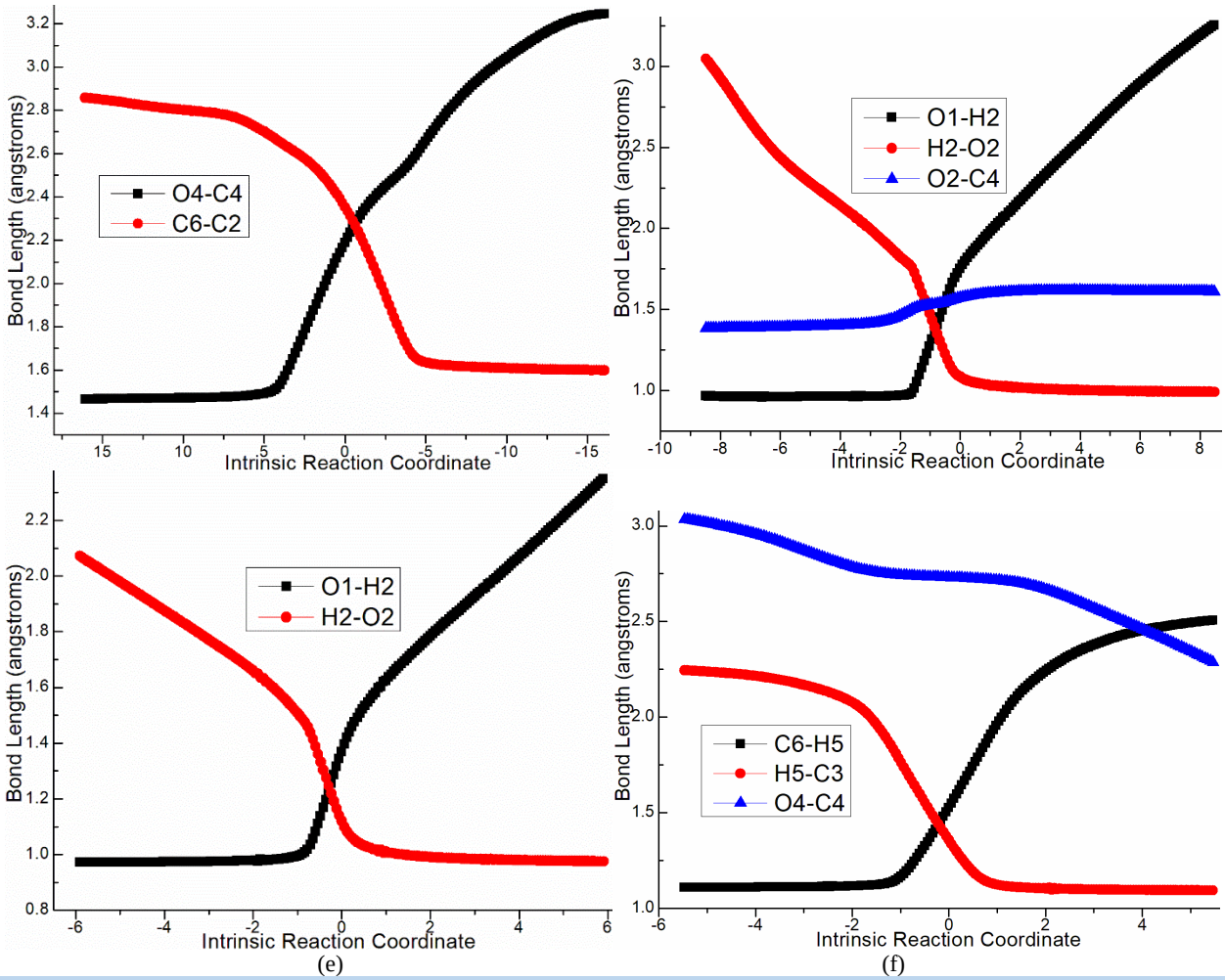

Figure S2. Highest Occupied Molecular Orbital (HOMO) of typical TSs. Different colors are used to identify the phase of the wave functions.